

In-depth analysis of site-specific N-glycosylation in vitronectin from human plasma by tandem mass spectrometry with immunoprecipitation

Heeyoun Hwang · Ju Yeon Lee · Hyun Kyoung Lee ·
Gun Wook Park · Hoi Keun Jeong · Myeong Hee Moon ·
Jin Young Kim · Jong Shin Yoo

Received: 31 July 2014 / Revised: 11 September 2014 / Accepted: 30 September 2014 / Published online: 6 November 2014
© Springer-Verlag Berlin Heidelberg 2014

Abstract The characterization of site-specific microheterogeneity in glycoprotein is very important for understanding cell biology and disease processes. Vitronectin is well known to be a multifunctional glycoprotein in the blood and the extracellular matrix, which is related to hepatocellular carcinoma (HCC). Here, we systematically analyzed the site-specific N-glycopeptides of vitronectin in human plasma by tandem mass spectrometry combined with immunoprecipitation and hydrophilic interaction liquid chromatography (HILIC) enrichment. Vitronectin was purified with immunoprecipitation by monoclonal antibody from plasma and digested to tryptic N-glycopeptides. Then, enrichment with HILIC materials was used and followed by analysis with nano-LC/MS/MS. The sequences of N-glycopeptides were identified from the mass spectra by high-energy C-trap dissociation (HCD) and collision-induced dissociation (CID). In HCD mode, oxonium ions were used for recognizing glycopeptides and γ ions for sequencing the peptide backbone. In CID mode, Y ions were used for characterizing their glycoforms. As a result, a total of

17 site-specific N-glycopeptides were completely identified in all of the three N-glycosylation sites of vitronectin in human plasma, including 12 N-glycopeptides first reported. Finally, we specifically found that three hybrid and four complex glycopeptides of triantennary forms with outer fucosylation increased in HCC human plasma.

Keywords Immunoprecipitation (IP) · Vitronectin · N-glycopeptides

Abbreviations

CID	Collision-induced dissociation
Fuc	Fucose
Gal	Galactose
GlcNAc	<i>N</i> -acetylglucosamine
HCC	Hepatocellular carcinoma
HCD	High-energy C-trap dissociation
HILIC	Hydrophilic interaction liquid chromatography
IP	Immunoprecipitation
Man	Mannose
N	Asparagine
Neu5Ac	<i>N</i> -acetyl neuraminic acid
NGSL~	NGSLFAFR
NISD~	NISDGFDPDNDVDAALALPAHSYSGR
NNAT~	NNATVHEQVGGPSLTSDLQAQSK

Heeyoun Hwang and Ju Yeon Lee contributed equally to this work.

Electronic supplementary material The online version of this article (doi:10.1007/s00216-014-8226-5) contains supplementary material, which is available to authorized users.

H. Hwang · J. Y. Lee · H. K. Lee · G. W. Park · H. K. Jeong ·
J. Y. Kim (✉) · J. S. Yoo (✉)
Mass Spectrometry Research Center, Korea Basic Science Institute,
Chungbuk, Republic of Korea
e-mail: jinyoung@kbsi.re.kr
e-mail: jongshin@kbsi.re.kr

J. Y. Lee · M. H. Moon
Department of Chemistry, Yonsei University, Seoul, Republic of
Korea

H. K. Lee · G. W. Park · H. K. Jeong · J. S. Yoo
Graduate School of Analytical Science and Technology, Chungnam
National University, Daejeon, Republic of Korea

Introduction

Glycosylation is one of the most common posttranslational modifications and is related to protein folding [1], quality control, sorting, degradation, and secretion. In glycosylation, glycans are attached to proteins that are related to the stabilization of the polypeptide folding structure [2], cell-cell adhesion, and signal transduction [3]. N-glycosylation happens at

the carboxy-amido nitrogen of the asparagine residues in the consensus tri-peptide sequence NXS/T, where X can be any amino acid except proline (N-glycosylation) [4]. O-glycosylation happens at the hydroxyl side chains of serine, threonine, and rarely in the hydroxyl-lysine or hydroxyl-proline residues [5]. Approximately 90 % of glycoproteins are likely to carry N-linked glycan, which is characterized as a high-mannose, a hybrid, and a complex type [6].

In general, high-performance liquid chromatography-mass spectrometry (HPLC-MS) techniques are preferable for the identification of glycosylation sites, the characterization of glycan composition, and isoform distribution [7–9]. However, analysis has remained a difficult task due to the low abundance of glycoproteins in complex biofluid samples, the microheterogeneity of glycan structures, the relatively low ionization efficiency in MS, and unsatisfied search tools for identification [10, 11].

In decades, to reduce sample complexity and to enrich glycoproteins, lectin-coupled enrichment [12–18], hydrazide chemistry [19, 20], hydrophilic interaction liquid chromatography (HILIC) separation [7, 21, 22], and so on were used [23–27]. In these studies, most methods were combined with PNGase F for the identification of released N-glycans from peptides and deglycosylated peptides. In this case, the composition of site-specific glycopeptide cannot be obtained because of loss of information on either glycans or peptides.

Recently, Pompach and his coworkers [28] isolated haptoglobin in human plasma by protein-protein interaction, enriched the glycopeptides, and examined the site-specific glycoform of haptoglobin where 60 N-glycopeptides were identified. This meant that they could analyze the various tryptic glycopeptides of haptoglobin in a complex sample such as human plasma. Meanwhile, immunoprecipitation (IP) or immuno-affinity purification has commonly been used for targeted protein analysis, by using the monoclonal antibody in human fluid samples or plasma.

Vitronectin is present in the blood and the extracellular matrix as a multifunctional glycoprotein and binds to various biological ligands such as collagen, plasminogen, and the urokinase receptor [29]. It is regulated by the blood systems related to complement, coagulation, and fibrinolysis [29–31]. In plasma, vitronectin, which is mostly synthesized by the liver, is related to chronic liver disease [32–35]. From the standard vitronectin, 15 glycans were identified and reported using a nonspecific digestion method by pronase [36]. Lee et al. reported two of the vitronectin glycopeptide NGSL~5_4_0_2 (Hex, *N*-acetylglucosamine (GlcNAc), fucose (Fuc), and *N*-acetyl neuraminic acid (Neu5Ac), respectively) and NISD~5_4_0_2 can be used as a hepatocellular carcinoma (HCC) biomarker [37, 38]. Recently, they addressed 12 N-glycopeptides in vitronectin increased in HCC plasma with multiple reaction monitoring (MRM) experiments [39]. Alternatively, eight glycopeptides of vitronectin

were identified by Mayampurath et al. in human serum with a high-throughput analysis, where they were limited to only two out of three N-glycosylation sites of vitronectin [40].

Here, we report a complete analysis of site-specific N-glycopeptides of vitronectin from standard and plasma samples. In order to pull down the vitronectin from plasma, its monoclonal antibody was applied, and HILIC was additionally used to enrich tryptic N-glycopeptides, followed by analysis with a nano-LC/Orbitrap mass spectrometer. Specially, collision-induced dissociation (CID) and high-energy C-trap dissociation (HCD) spectra were systematically interpreted for in-depth comparison of the glycopeptides in vitronectin between normal and HCC plasma.

Materials and methods

Materials

Dithiothreitol (DTT), iodoacetamide (IAA), and formic acid were purchased from Sigma-Aldrich (St. Louis, MO). For proteome digestion, trypsin from Promega (Madison, WI) was used. A ZIC-HILIC kit (Proteo Extract Madison, WI) was purchased for glycopeptide enrichment. Deionized water was prepared with a Millipore system (Millipore, Eugene, OR), and HPLC grade acetonitrile was obtained from J.T. Baker (Phillipsburg, NJ). Vitronectin standard from human (V8379) was purchased (Sigma-Aldrich, St. Louis, MO) for the analysis.

Methods

Plasma sample preparation

Plasma samples were used with informed consent and in accordance with the IRB guidelines from Yonsei University College of Medicine (Seoul, Republic of Korea). Human plasma samples came from healthy donors or HCC cancer patients, and each was divided into four bags of equal volume with an appropriate concentration of K₂EDTA. Each aliquot was frozen and stored at –80 °C until use.

Depletion of major abundant proteins from human plasma

The six most abundant proteins (albumin, sero-transferrin, IgG, IgA, haptoglobin, and α_1 -antitrypsin) of human plasma were depleted with a multiple affinity removal column (MARC; Agilent) equipped with a HP1100LC system (Agilent). Each crude 20 μ L human plasma sample was diluted with 80 μ L of buffer A containing the proper amount of protease inhibitor (Complete Protease Inhibitor Cocktail tablet (Roche, Indianapolis, IN)). Seventy to 100 μ L of the diluted solution was centrifuged with a 0.22 μ m filter

(16,000×g, room temperature, 1–2 min) and injected into a multiple affinity removal column (flow rate=0.25 mL min⁻¹). Flow-through fractions from MARC were used or stored at -20 °C before use. The depleted plasma sample was added in 10,000 Da molecular weight cutoff (MWCO) VIVASPIN filters (product VS0602; Sartorius, Göttingen, Germany).

Vitronectin immunoprecipitation and digestion

For the immunoprecipitation of vitronectin in plasma, the Dynabeads MyOne™ Tosyl-activated (Invitrogen, Carlsbad, CA, USA) cross-linked with vitronectin monoclonal antibody (mAb) was prepared according to the protocol supplied by the manufacturer. Briefly, 100 µL of beads washed once with coating buffer (0.1 M sodium borate, pH 9.5) were added to 695 µL of coating buffer. After mixing properly, 40 µg of vitronectin mAb (Santa Cruz Biotechnology, Dallas, TX, USA) was added and mixed. Before incubating for 16 h at 37 °C with a slow tilt rotation, 415 µL of 3 M ammonium sulfate stock solution was added. After removing the supernatant on the magnet, 1250 µL of blocking buffer (PBS pH 7.4 with 0.5 % BSA and 0.05 % Tween-20) was added and incubated overnight at 37 °C at a slow tilt rotation. After removing the supernatant on the magnet, it was washed three times with washing and storage buffer (PBS pH 7.4 with 0.1 % BSA and 0.05 % Tween-20). For vitronectin purification, 100 µg of depleted human plasma samples of normal (10 pooled) and HCC (10 pooled) were added to the vitronectin mAb (Santa Cruz Biotechnology, Dallas, TX) cross-linked beads and incubated at 4 °C overnight, under gentle mixing conditions. After washing (three times with PBS), immunocomplex and standard purchased vitronectin were resuspended in 100 µL of 50 mM ammonium bicarbonate and 5 µL of 200 mM DTT and were incubated at 60 °C for 30 min. After alkylation by 20 µL of 100 mM IAA in darkness at room temperature for 30 min, the immunocomplex was digested by trypsin at 37 °C overnight. After quenching, tryptic digests were dried using a SpeedVac and redissolved in 0.1 % formic acid in water prior to HILIC.

Glycopeptide enrichment with HILIC

A ZIC-HILIC kit (Proteo Extract® Glycopeptide Enrichment Kit) was used for the glycopeptide enrichment of vitronectin from the pooled normal and HCC plasma. The enrichment was performed according to the manufacturer's instructions (EMD Millipore). The purified and digested vitronectin was diluted by adding 50 µL ZIC® Binding Buffer, and then 50 µL ZIC® Glycocalcure Resin was transferred to a new e-tube. The tube that contained the 50 µL ZIC® Glycocalcure Resin was centrifuged for 1–2 min at 2000–2500×g, and then the supernatant was completely removed and discarded. The diluted digest sample was added to the ZIC® Glycocalcure

Resin and mixed and incubated at 1200 rpm for 10–20 min. The tube was centrifuged for 1–2 min at 2000–2500×g. The supernatant was then completely removed. The ZIC® Glycocalcure Resin was totally washed three times with 150 µL ZIC® Wash Buffer. Seventy-five to 100 µL of ZIC® Elution Buffer was added for glycopeptide elution. The tube was mixed, incubated at 1200 rpm for 2–5 min, and centrifuged for 1–2 min at 2000–2500×g. The supernatant containing glycopeptides was transferred in a new e-tube and centrifuged for 2 min at 10,000×g. Elutes were dried in a SpeedVac and redissolved in 0.1 % formic acid in water for UPLC/LTQ Orbitrap Elite mass spectrometry analysis.

Nano LC-ESI-MS/MS and proteome search

Trypsin-digested standard vitronectin and HILIC-enriched glycopeptides from plasma were analyzed using a NanoAcquity UPLC system (Waters, USA) and an LTQ Orbitrap Elite mass spectrometer (Thermo Scientific, USA) equipped with a nano-electrospray source. Aliquots, each 5 µL, of the peptide solution were loaded into an autosampler and were desalted and concentrated on a C₁₈ trap column of i.d. 180 µm, length 20 mm, and particle size 5 µm (Waters, USA) at a flow rate of 5 µL min⁻¹ for 10 min. The trapped peptides were back-flushed and separated on a homemade microcapillary C₁₈ analytical column of i.d. 100 µm and length 200 mm (particle size 3 µm, 125 Å). The LC gradient was started with a 5 % mobile phase B (A—100 % water with 0.1 % formic acid and B—100 % acetonitrile (ACN) with 0.1 % formic acid). The mobile phase B was kept at 5 % for 15 min and then was linearly ramped up to 15 % B over 5 min, to 50 % B over 75 min, and to 95 % B over 1 min. The 95 % mobile phase B was maintained for 13 min. After that, the mobile phase B was descended to 5 % over 1 min and maintained there for 10 min before the next run, and then 2.2 kV was applied to produce the electrospray. The LTQ Orbitrap Elite was operated in a data-dependent mode during the chromatographic separation. Five data-dependent MS/MS scans were obtained by CID with a 10 ms activation time and HCD with a 30 ms activation time (Rs, 15,000) per each full scan (Rs, 120,000) for identification of glycopeptides. Thirty-five percent of normalized collision energy (NCE) in CID and HCD was applied. Previously fragmented ions were excluded for 180 s for all MS/MS scans. Label-free quantitation was performed from XIC with a 10 ppm tolerance. For the nonglycopeptide identification, the raw files from each analysis of flow-through from the HILIC enrichment step were processed into a .dta file. The resulting *.dta files were processed against the International Protein Index (IPI) Human database (version 3.22; 57,846 sequences; 26,015,783 residues) using the Integrated Proteomics Pipeline (IP2) search engine (version 1.01; Integrated Proteomics Application Inc., USA). The IP2 was used with monoisotopic mass selected, a

precursor mass tolerance of 50 ppm, and a fragment mass tolerance of 600 ppm. Trypsin was selected as the digestion enzyme, with one potential missed cleavage. Oxidized methionine and carbamidomethylated cysteine were chosen as variable modifications for identifying nano-UPLC/Orbitrap MS/MS results in DDA mode.

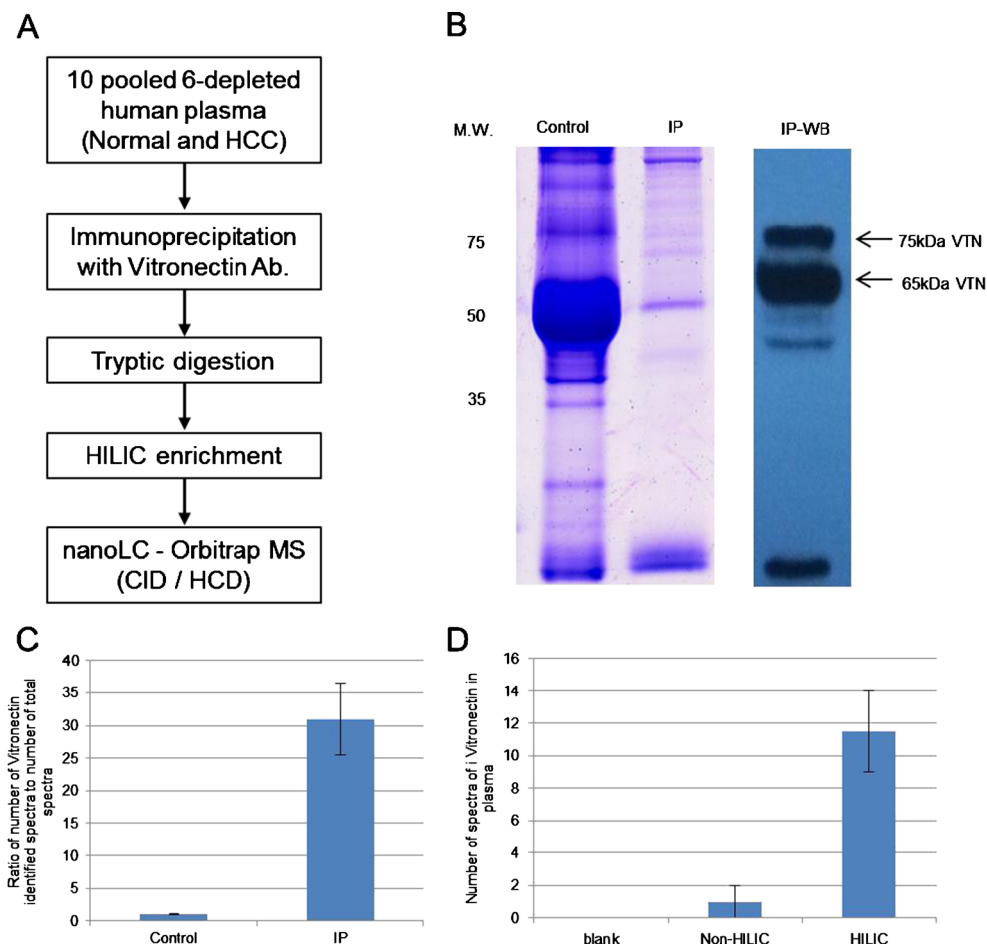
Results and discussion

Immunoprecipitation and HILIC enrichment in human plasma

The glycoprotein concentration in plasma was shown to be in a dynamic range from 1 mg mL⁻¹ to 1 ng mL⁻¹ [41]. The concentration of vitronectin was known to be about 500 ng mL⁻¹ using mass-based quantitation methods with selective reaction monitoring [41]. In addition, using specific antibody, the immunoprecipitation technique has been commonly used for enrichment-targeted proteins in complex biological samples like human plasma. Ten pooled and top six depleted human plasma from normal and HCC samples were prepared for vitronectin immunoprecipitation, HILIC

enrichment, and nano-LC/Orbitrap mass spectrometry (Fig. 1A). Because vitronectin has three N-glycosylation sites (Sup. Fig. 1), site-specific N-glycopeptide analysis was needed rather than total glycan analysis with PNGase F. Vitronectin was pulldown using monoclonal antibody from human plasma, and SDS-PAGE and Western blot analysis were performed (Fig. 1B). As a result, the vitronectin in the plasma was detected in two bands, at 65 and 75 kDa. It was reported that vitronectin exists in two forms: as a single chain (75 kDa) and as a clipped form (65 and 10 kDa) in human plasma [42, 43]. Furthermore, before HILIC enrichment, a proteome search of vitronectin was performed with a proteome database search engine. It showed that the number of spectra counts for elutes from vitronectin IP were 35 times higher than those of the total serum control (Fig. 1C). It was clear that the vitronectin proteins were well immunopurified and used for the next steps. Then, the tryptic-digested glycopeptides were enriched by HILIC, which was widely used for glycan and glycopeptides [44–47]. Using a nano-LC Orbitrap tandem MS, following the analysis of glycopeptide with HCD and CID spectra, it was shown that vitronectin glycopeptides were eight times more prevalent in HILIC than blank and non-HILIC in human plasma (Fig. 1D). Therefore, it was

Fig. 1 (A) A scheme of glycopeptide analysis with the immunoprecipitation and HILIC enrichment of vitronectin in human plasma. (B) Seventy-five and 65 kDa of immunoprecipitated vitronectin were detected by CBB stain and Western blot, respectively. (C) The ratio of the number of vitronectin-identified spectra to the number of total spectra was calculated in the human serum control and IP elutes from the protein search results. (D) HILIC enrichment effects of tryptic glycopeptide from human vitronectin. The quantity of the identified vitronectin glycopeptide spectra was detected with nano-LC MS/MS Orbitrap. Blank means a negative control in which the IP and HILIC enrichment were performed without Ab



confirmed that HILIC enrichment could be a useful method for glycopeptide enrichment in this study.

Systematic glycopeptide identification with hybrid tandem MS (HCD and CID)

Recently, the experimental conditions of HCD and CID modes of Orbitrap hybrid mass spectrometry were reported to optimize the detection of N-glycosylation sites and the microheterogeneity of glycans attached to the glycopeptides [48]. Here we tried a systematic identification of tryptic N-glycopeptides using tandem mass spectrometry with combination of CID and HCD modes.

Glycopeptide spectra selection in HCD

First, for the manual identification, HCD spectra that have oxonium ion peaks were used for the selection of glycopeptide candidates from the digested peptide mixture of glycoprotein (Fig. 2A). The theoretical m/z of the six oxonium ions from GlcNAc (m/z 138.05, m/z 168.05, and m/z 204.09), NeuAc (m/z 274.09 and m/z 292.09), and GlcNAc-Hex (m/z 366.08) in glycopeptides from

HCD mass spectrometry were well known [49, 50]. In our study, we selected the glycopeptide candidates with at least four ions out of six oxonium ions.

Second, from the tryptic glycopeptide candidates selected, we considered b/y series ions from peptide backbone and Y series ions including Y0, Y1, and the cross-ring cleavage ion of GlcNAc that lost 120.0423 Da from Y1 in HCD spectra (Fig. 2A). Additionally, we listed and calculated the theoretical molecular weight (M.W.) of N-glycopeptide retrosynthesized with targeted tryptic peptide and 331 N-glycans from human serum [51]. Then, we matched the M.W. of the parent ions from selected candidates by Y series ions to the M.W. of the retrosynthetic N-glycopeptide list with 10 ppm tolerance (Fig. 2A).

Classification of glycopeptide microheterogeneity in CID

For the characterization of target glycopeptide, the fragments of candidate glycopeptides were assigned against the predicted list in CID tandem mass spectrometry. For the classification of N-glycopeptide by our algorithm, the core ion which is PEP_3_2_0_0 was used as the central fragments. Then, we checked the fragmented ions of the core +162 Da and/or the

Fig. 2 A scheme of systematic glycopeptide identification with CID and HCD spectra. **(A)** Selection of glycopeptide with oxonium ions and identification of targeted glycopeptide with Y0, Y1, and Y1-120 Da or b/y series ions in HCD spectra. **(B)** Classification algorithm of microheterogeneity of glycopeptide in CID spectra. Core means a fragmented ion of PEP_3_2_0_0 from the parent glycopeptide. Peptide (PEP), ●; mannose, ●; galactose, ■; N-acetylglucosamine, ▲; fucose, ◆; sialic acid

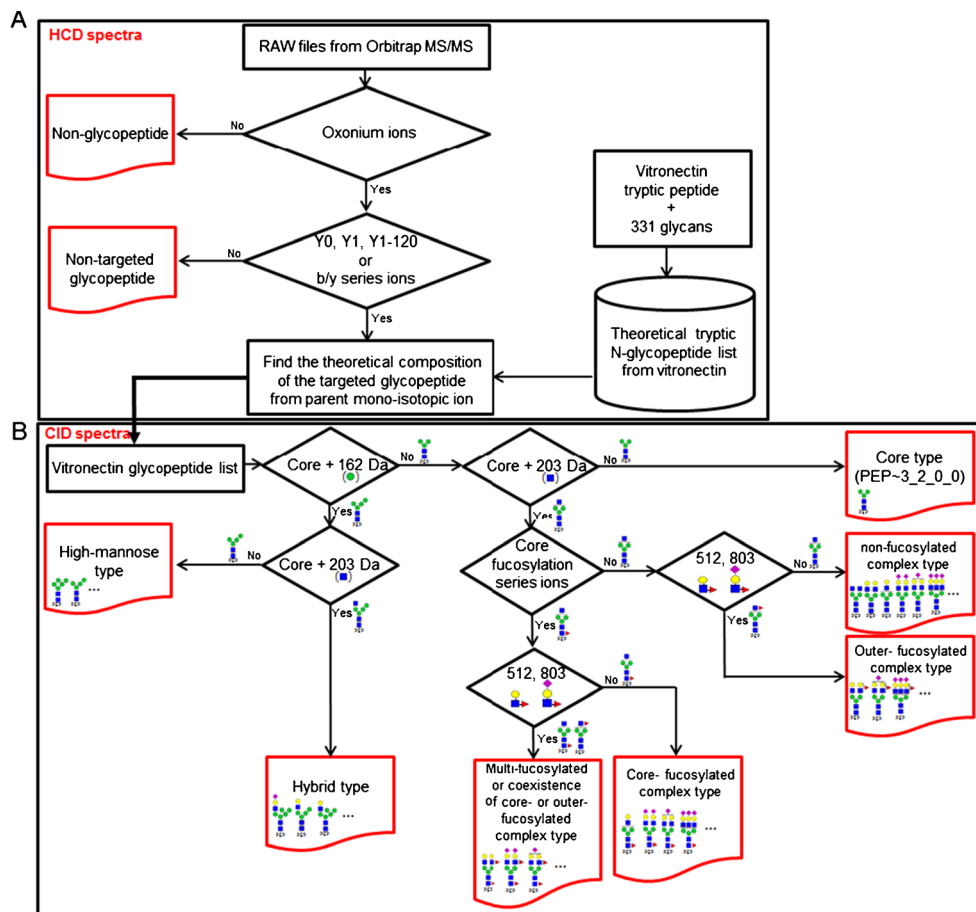


Table 1 Identified glycopeptides from vitronectin in standard protein and human plasma




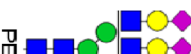




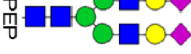
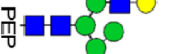




Glycopeptides	Structure	Theo. m/z (charge)	Exp. m/z (charge)	ppm	RT	Std.	Plasma (Normal / HCC)		New or Reported	
							Std.	Plasma		
(86) NN*ATVHEQVGGPSLTSDLQAQSK										
PEP-5_4_0_1		1432.285(+3)	1432.287(+3)	-1.49	55.92	√	n.d.	n.d.	(2)	n.d.
PEP-5_4_0_2		1529.316(+3) 1147.241(+4)	1529.316(+3) 1147.241(+4)	0.00 0.00	57.03	√	√	√	(2)(3)	New
PEP-6_5_0_3		1131.298(+4)	1311.298(+4)	0.00	62.88	√	√	n.d.	(3)	New
PEP-6_5_1_3		1347.812(+4)	1347.812(+4)	0.00	62.84	n.d.	n.d.	√	(3)	New
(169) N*GSLFAFR										
PEP-4_3_0_1		1230.513(+2) 820.676(+3)	1230.511(+2) 820.677(+3)	1.38 -1.21	68.23	√	n.d.	√	(2)	New
PEP-5_3_0_0		1165.988(+2)	1165.992(+2)	-3.68	67.09	√	n.d.	√	(2)	New
PEP-5_3_0_1		1311.539(+2) 874.694(+3)	1311.537(+2) 874.694(+3)	1.52 0.00	68.07	√	√	√	(2)	(1)
PEP-5_4_0_1		942.388(+3)	942.387(+3)	1.06	67.78	√	√	√	(2)	New
PEP-5_4_0_2		1558.624(+2) 1039.420(+3)	1558.626(+2) 1039.419(+3)	-1.28 0.96	65.99	√	√	√	(2)(3)	(1)
PEP-6_3_0_0		1247.016(+2)	1247.017(+2)	-0.80	59.46	√	n.d.	n.d.	New	n.d.
PEP-6_3_0_1		1392.563(+2) 928.711(+3)	1392.565(+2) 928.713(+3)	1.43 -2.15	62.67	√	n.d.	√	(2)	New
PEP-6_5_0_3		1258.161(+3)	1258.161(+3)	0.00	68.20	√	√	n.d.	New	New
PEP-6_5_1_2		1209.815(+3)	1209.816(+3)	0.82	65.17	√	n.d.	n.d.	(3)	n.d.
PEP-6_5_1_3		1306.847(+3)	1306.849(+3)	-1.53	68.65	√	n.d.	√	(3)	New

Table 1 (continued)

Glycopeptides	Structure	Theo. m/z (charge)	Exp. m/z (charge)	ppm	RT	Std.	Plasma (Normal / HCC)		New or Reported	
							Std.	Plasma	Std.	Plasma
(242) N*ISDGFDFGIPDNVDAALALPAHSYSGR										
PEP~5_4_0_0		1099.481(+4)	1099.481(+4)	0.00	69.27	√	n.d.	n.d.	New	n.d.
PEP~5_4_0_1		1172.253(+4) 938.004(+5)	1172.253(+4) 938.005(+5)	0.00 1.07	71.01	√	√	√	(2)	New
PEP~5_4_0_2		1245.029(+4) 996.223(+5)	1245.027(+4) 996.223(+5)	1.60 0.00	72.64	√	√	√	(2)(3)	(1)
PEP~5_4_1_0		1135.994(+4)	1135.995(+4)	0.88	69.22	√	n.d.	n.d.	New	n.d.
PEP~5_4_1_1		1208.768(+4) 967.216(+5)	1208.769(+4) 967.216(+5)	-0.82 0.00	70.77	√	n.d.	n.d.	New	n.d.
PEP~5_4_1_2		1281.544(+4)	1281.542(+4)	1.56	72.57	√	√	n.d.	(2)(3)	(1)
PEP~6_5_0_0		1190.763(+4)	1190.763(+4)	0.00	69.22	√	n.d.	n.d.	New	n.d.
PEP~6_5_0_1		1263.536(+4) 1011.031(+5)	1263.536(+4) 1011.031(+5)	0.00 0.00	70.60	√	n.d.	n.d.	New	n.d.
PEP~6_5_0_2		1336.310(+4) 1069.249(+5)	1336.312(+4) 1069.250(+5)	-1.49 0.93	72.39	√	n.d.	n.d.	(2)	n.d.
PEP~6_5_0_3		1409.086(+4) 1127.468(+5)	1409.086(+4) 1127.469(+5)	0.00 0.89	73.62	√	n.d.	√	(3)	(1)
PEP~6_5_1_1		1300.051(+4) 1040.242(+5)	1300.052(+4) 1040.242(+5)	-0.77 0.00	70.59	√	n.d.	n.d.	New	n.d.
PEP~6_5_1_2		1372.827(+4) 1098.461(+5)	1372.824(+4) 1098.461(+5)	0.00 0.00	72.33	√	n.d.	√	New	New
PEP~6_5_1_3		1445.601(+4) 1156.680(+5)	1445.601(+4) 1156.681(+5)	0.00 -0.86	74.48	√	n.d.	√	(3)	(1**)
PEP~6_5_2_3		1185.891(+5)	1185.893(+5)	-1.68	74.26	√	n.d.	n.d.	New	n.d.

(1) Mayampurath et al. [40], human Serum; (2) Hua et al. [36], standard vitronectin; (3) Lee et al. [39], standard vitronectin

* N-glycosylation site

** Core-fucosylated form was reported in Mayampurath et al.

New, newly identified glycopeptides in this report; PEP peptide, ●; mannose, ●; galactose, ●; N-acetylglucosamine, ■; fucose, ▲; N-acetylneuraminic acid; n.d. not detected

core +203 Da and classified the glycopeptide as a high-mannose, a hybrid, or complex type (Fig. 2B).

Next, we considered the fucosylation of complex-type glycopeptide (Fig. 2B). At least in humans, the fucose could be attached at an outer arm GlcNAc (the alpha 1-3 or 1-4 linkage) and/or galactose (Gal) (alpha 1-2 linkage), and at core GlcNAc (the alpha 1-6 linkage), which is linked with the asparagine of the glycosylation site. Recently, the microheterogeneity of core and/or outer fucosylation has been characterized using high-resolution mass spectrometry with various MS/MS fragmentations [28, 52, 53]. For the classification of fucosylated glycopeptide, first, GlcNAc-Fuc and its neutral loss ion were suggested as the indicator ion with reliability of the core fucosylation [52, 53]. Second, 512.3633 (●) and 803.5337 (●) oxonium ions were considered that were fragmented from the outer arm fucose of N-glycopeptide in CID [28]. According to the existence and relative abundance of these indicator ions, the microheterogeneity of core and outer fucosylation could be characterized by our algorithm (Fig. 2B).

Systematic glycopeptide characterization of standard vitronectin

Vitronectin has three N-glycosylation sites such as NNATVHEQVGGPSLTSDLQAQSK (NN⁸⁶AT~), N G S L F A F R (N¹⁶⁹G S L ~), and NISDGFDPDNDVAALALPAHSYSGR (N²⁴²ISD~). A recent study reported 15 glycopeptides from standard vitronectin by the pronase, a nonspecific digestion enzyme [36]. Before the analysis of the plasma sample, we analyzed the standard vitronectin that was purchased from the manufacturer. Prepared vitronectin standard protein was reduced, alkylated, tryptic-digested, and then analyzed by nano-LC/Orbitrap MS/MS with CID and HCD. Using our algorithm, we considered total 993 numbers of retrosynthesized N-glycopeptides from three N-glycosylation sites of vitronectin (Sup. Excel Table 1). Then, N-glycopeptide structure was chosen and classified by our algorithm from selected candidates in the list of retrosynthesized N-glycopeptides.

As a result, 27 glycopeptides were characterized from the three N-glycosylation sites of vitronectin including 10 newly found glycopeptides (Table 1). Most were characterized as biantennary or triantennary glycopeptides that were complex-type glycopeptides. Representatively, in the NNAT~_{5_4_0_2}, NGSL~_{4_3_0_1}, and NISD~_{5_4_0_2} glycopeptides, almost all highly intense peaks were well assigned as fragment ions in HCD and CID (Fig. 3, Sup. Fig. 2).

Vitronectin glycopeptide selection by the y and Y series ions in HCD

Specifically, y series ions from the peptide backbone were mainly observed in two sites (NN⁸⁶AT~ and N²⁴²ISD~,

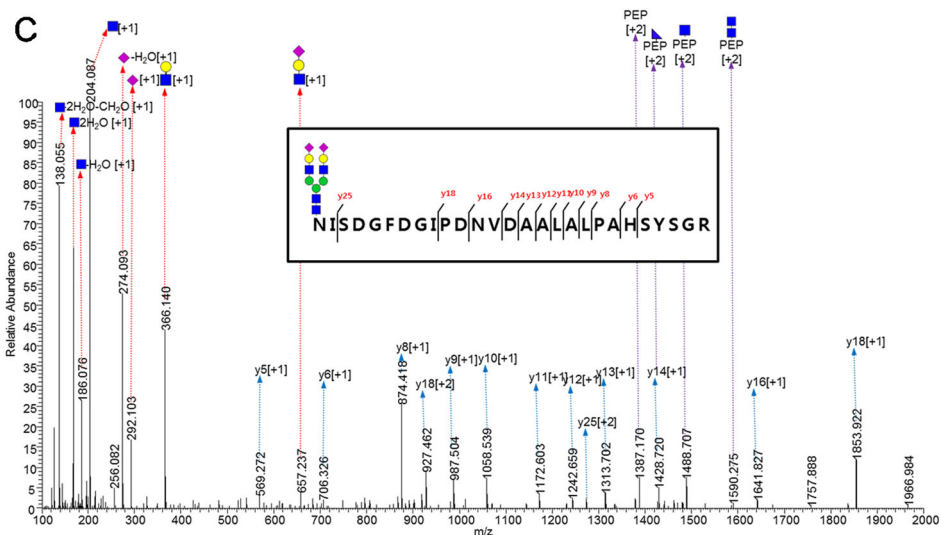
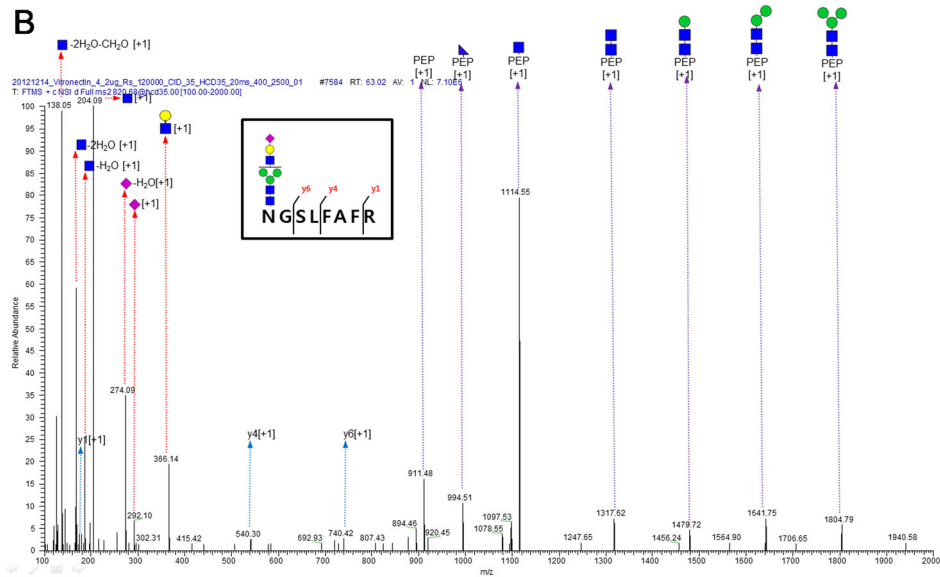
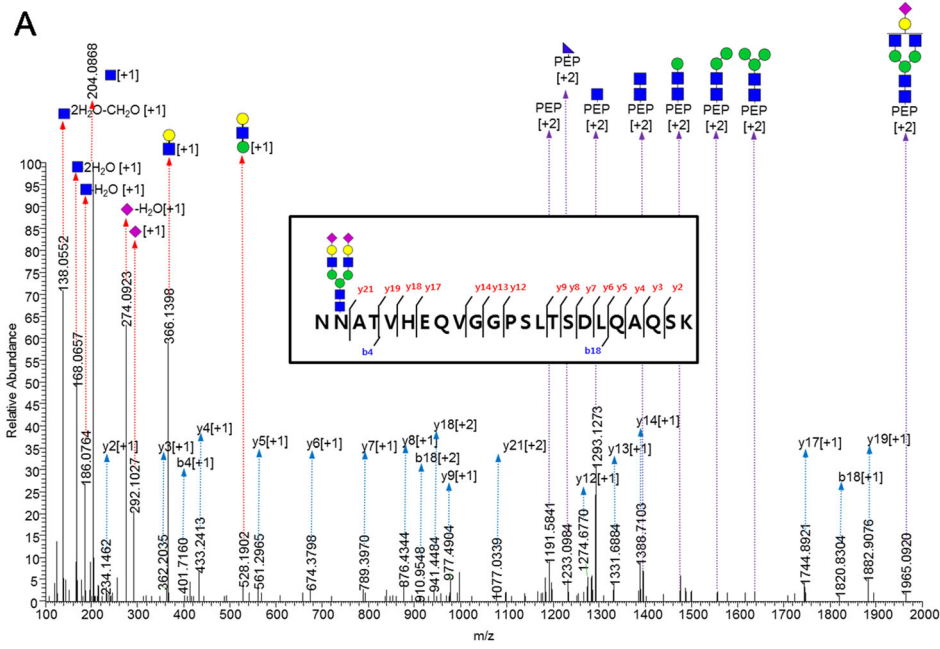
respectively) of the HCD spectrum (Fig. 3A, C) and increased the identification confidence of glycopeptides. The HCD fragmentation of glycopeptides in a C-trap commonly occurred with a high mass accuracy; thus, the cleavages of mono-, di-, or trisaccharides from their glycosidic bonds were observed in the low *m/z* cutoff [48–50, 54]. Representatively, the glycosylation site of NNAT~_{5_4_0_2} (1147.2409 (+4)) is adjacent to the N-terminus. Therefore, the y series ions that did not include the glycosylation site were more dominant in the HCD spectrum than the b series ions contained in the N-site (Fig. 3A, C).

The other hand, the tryptic peptide sequence from N¹⁶⁹GSL~ was shorter than those from either the NN⁸⁶AT~ or N²⁴²ISD~. Therefore, in these HCD spectra from N¹⁶⁹GSL~ glycopeptides, the glycan-fragmented glycopeptide ions (Y ions) corresponding to the glycosidic bond cleavages of the sugar chain were more readily detected than the y series ions from the peptide backbone (Fig. 3B). Therefore, HCD fragmentation patterns differ according to the length of their peptide sequence, the location of the N-glycosite, and the complexity of their glycan structure at the peptide backbone.

The classification of hybrid- and complex-type glycopeptide in CID

Using our algorithm, most glycopeptides from vitronectin were well characterized as a complex type in all three sites. Otherwise, the identified hybrid types that had both noncleaved mannoses and GlcNAc with core structure, NGSL~_{5_3_0_0}, NGSL~_{5_3_0_1}, and NGSL~_{6_3_0_1} were identified from only the N¹⁶⁹GSL~ site (Table 1). In these, NGSL~_{5_3_0_1} was compared to the NGSL~_{5_4_0_1} complex-type glycopeptide, representatively (Sup. Fig. 3). The hybrid-specific fragments such as 5_2_0_0 (*m/z* 1217.5673 (+1)), 5_2_0_1 (*m/z* 1508.7395 (+1)), NGSL~_{4_2_0_0} (*m/z* 983.7921 (+2)) and *m/z* 1966.0780 (+1)), and NGSL~_{5_3_0_0} (*m/z* 1166.2695 (+2)) were observed in the CID spectra from NGSL~_{5_3_0_1}. On the other hand, these hybrid-specific oxonium and fragmented glycopeptide ions were not detected in the CID spectrum of NGSL~_{5_4_0_1} glycopeptide classified as complex type. In addition, these unique ions of hybrid type were well detected in other hybrid type glycopeptides, NGSL~_{5_3_0_0} and NSGL~_{6_3_0_1} (Sup. Fig. 3).

Fig. 3 HCD spectrum of the identified glycopeptide from vitronectin in human plasma. The red arrow indicates oxonium ion, the light blue indicates y series ions fragmented from the peptide. Purple indicates the Y series fragment ions from the glycopeptide. ▲ cross-ring cleavage fragments of GlcNAc with loss of 120.05 Da. (A) HCD spectrum of NNAT~_{5_4_0_2}. (B) HCD spectrum of NGSLFAFR~_{4_3_0_1}. (C) HCD spectrum of NISD~_{5_4_0_2}



The classification of fucosylated glycopeptides in CID

In the CID spectrum of NISD~_5_4_1_2 with 35 % dissociation energy, six pairs of afucosylated and fucosylated fragment ions including GlcNAc-Fuc and its neutral loss ion were detected (Sup. Fig. 4A). Besides, outer fucosylation indicators were not detected in this glycopeptide, which was classified as core-fucosylated glycopeptide. The other hand, NISD~_6_5_1_2 and NISD~_6_5_1_3 were classified as outer fucosylated glycopeptide, because they had the low intensity of core-fucosylated indicator ions and relatively high intensity of 512.3633 (●) and 803.5337 (●) oxonium ions (Sup. Fig. 4B, C). Additionally, the coexistence of core and outer fucosylation is possible in the same identified N-glycopeptide [28]. NISD_6_5_2_3 was characterized as a dual-fucosylated glycopeptide which had indicator ions of both core and outer fucosylation (Sup. Fig. 4D). Although the possibility of their coexistence or rearrangement [55] could not be considered, the core-fucosylated and outer fucosylated glycopeptides could be characterized. In summary, pair fragment ions of core-fucosylated glycopeptide and 512.3633 (●) and 803.5337 (●) oxonium ions from outer fucosylated glycopeptide were suggested as the indicator of microheterogeneity in fucosylated N-glycopeptide characterization in CID spectra.

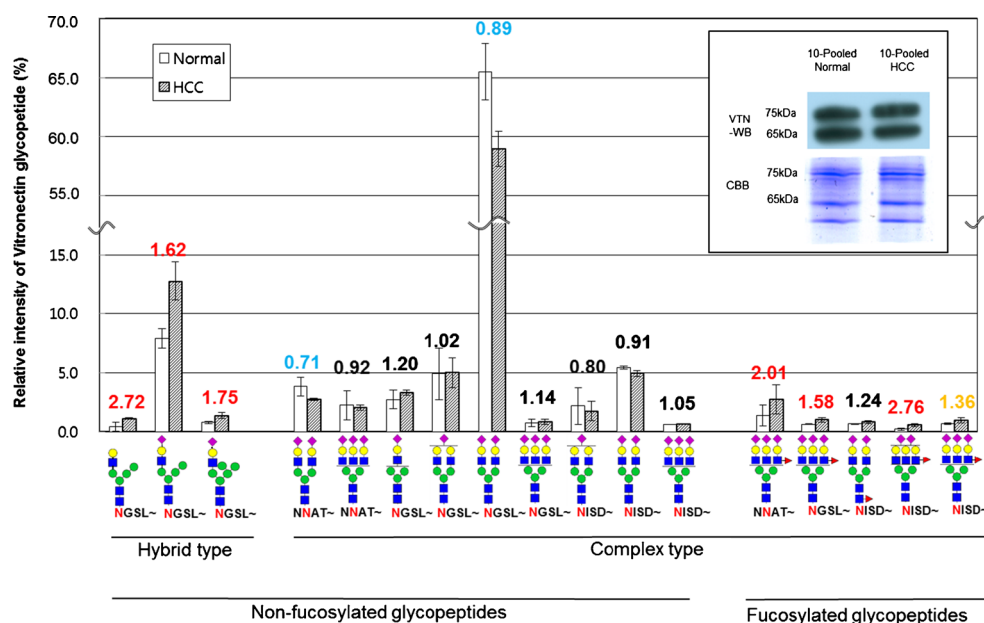
Characterization of vitronectin glycopeptides in normal and HCC human plasma

In human plasma, a total of 17 glycopeptides were identified with IP and HILIC enrichment including 12 newly found from the three N-glycosylation sites (Table 1, Sup. Fig. 5). These

included seven glycopeptides that were reported by Mayampurath et al., except that only one had a lactose-amine tail (N¹⁶⁹GSL~, PEP_5_4_0_1) [40]. However, we identified the glycopeptide with the same M.W. as the complex type (Table 1, Sup. Fig. 2). In 17 glycopeptides, 3 hybrid- and 14 complex-type glycopeptides were characterized including one core-fucosylated and four outer fucosylated glycopeptides, using HCD and CID tandem MS spectrometry (Table 1).

The area of extracted ion chromatogram (XIC) with 10 ppm mass tolerance for each glycopeptide was used for quantitation between the normal and HCC plasma samples. Then global normalization in the area of total vitronectin glycopeptide XIC was performed (Fig. 4). The relative average intensity of HCC to normal was calculated, and the highest CV of the HCC to normal ratio was <30 %. In each of the three N-sites, PEP_5_4_0_2, biantennary complex-type glycan was dominantly detected. In addition, we found that three hybrid-type and four fucosylated glycopeptides were increased over 1.5-fold in the HCC plasma (Fig. 4). Meanwhile, the Western blot analysis showing the total protein levels of vitronectin indicated very similar results between the normal and HCC plasma, which each comprised the pooled samples from 10 individuals (Fig. 4, upper panel). This means that the total vitronectin levels could not show any difference, but the outer fucosylated glycopeptides could be considered as the biomarker candidates. The Fut 6 and Fut 8 genes, which code fucosyltransferase and are related to the fucosylation of glycan, were reported with increased mRNA and protein level in HCC liver tissue [56–59]. Recently, it was also reported that fucosylated glycopeptide of vitronectin was relatively increased in cancer [39, 60]. Using an AAL lectin-coupled MRM method, we reported that the aberrant

Fig. 4 Relative intensity of the vitronectin glycopeptides from the normal human and HCC plasma aliquots. However, the vitronectin abundance in the Western blot showed no difference between the normal and HCC plasma (*in the panel*). The three hybrid-type glycopeptides and four outer fucosylated glycopeptides were increased in HCC plasma (*in the graph*). The number in the graph indicated the ratio of glycopeptide abundance of HCC vs. normal



fucosylated glycosylation of protein was increased in HCC plasma with no change of protein level [12]. In contrast, the hybrid-type glycopeptide was found at only one site, N169. It is reported that the Golgi alpha mannosidase 2 was suppressed in the HCC, which is related to the hybrid-type pathway [61]. However, there is still a challenge, which is related to the enzyme activity in the glycosylation pathway of proteins, and it has to explain why the site-specific hybrid type of vitronectin was increased in HCC plasma.

Conclusions

In complex human plasma samples, the analysis of glycopeptides with microheterogeneities from various proteins is still a challenging work. We report that IP and HILIC could be a good solution for enrichment of low abundant glycopeptides. Using these enrichment techniques, glycopeptides were fully characterized from three N-glycosites (N86, N169, and N242) of vitronectin from human plasma. In HCD spectra from high-resolution tandem MS, the selection of oxonium ions and γ and Y series ions of glycopeptides improves the confidence for identification of vitronectin. In CID spectra, the structural information from Y series ions was enough for the characterization of its glycopeptides. As a result, 27 N-glycopeptides were characterized from human standard vitronectin including 10 newly found, where 14 complex- and 3 hybrid-type glycans were identified in plasma. Comparing previous reports, we identified more numbered and site-specific glycopeptides. Lee et al. reported that two fucosylated glycopeptides increased in HCC plasma and were suggested as a HCC biomarker [39]. Including these glycopeptides, we propose that three hybrid and four outer fucosylated glycopeptides could be candidates for biomarker developments in HCC. On the other hand, two complex types of vitronectin, NNAT~5_4_0_2 and NGS~5_4_0_2, decreased in HCC. In this discrimination between nonfucosylation and outer fucosylation of complex-type glycopeptide in vitronectin, we carefully suggested that complex glycan of 5_4_0_2 in N-sites of vitronectin could be more branched and outer fucosylated in HCC. The *N*-acetylglucosaminyltransferases V (GnT-V), which are related in branched glycosylation, and fucosyltransferase 6, which is related in outer fucosylation of N-glycan, are increased in liver cancer samples [56, 62, 63]. Although the human plasma is one of the most complex samples with a wide dynamic concentration range, the glycopeptide analysis of the vitronectin was practically possible through the IP and HILIC enrichment with tandem mass spectrometry. Furthermore, our in-depth analysis of glycopeptides would suggest new insight for the study of low abundant glycoprotein in complex matrix.

Acknowledgments The research was supported by the Korea Health Technology R&D Project through the Korea Health Industry Development Institute (KHIDI), funded by the Ministry of Health & Welfare, Republic of Korea (grant number: HI13C2098); the research program through the Korea Basic Science Institute (grant number: D34413, T34750); and the Proteogenomic Research Program, through the National Research Foundation (NRF) funded by the Ministry of Science, ICT & Future Planning (NRF-2013M3A9B9044431).

References

1. Parodi AJ (2000) Protein glucosylation and its role in protein folding. *Annu Rev Biochem* 69:69–93
2. Helenius A, Aebi M (2004) Roles of N-linked glycans in the endoplasmic reticulum. *Annu Rev Biochem* 73:1019–1049
3. Varki A (1993) Biological roles of oligosaccharides: all of the theories are correct. *Glycobiology* 3:97–130
4. An HJ, Peavy TR, Hedrick JL, Lebrilla CB (2003) Determination of N-glycosylation sites and site heterogeneity in glycoproteins. *Anal Chem* 75:5628–5637
5. Walsh G, Jefféris R (2006) Post-translational modifications in the context of therapeutic proteins. *Nat Biotechnol* 24:1241–1252
6. Kornfeld R, Kornfeld S (1985) Assembly of asparagine-linked oligosaccharides. *Annu Rev Biochem* 54:631–664
7. Neue K, Mormann M, Peter-Katalinić J, Pohlentz G (2011) Elucidation of glycoprotein structures by unspecific proteolysis and direct nano ESI mass spectrometric analysis of ZIC-HILIC-enriched glycopeptides. *J Proteome Res* 10:2248–2260
8. Pan S, Chen R, Aebersold R, Brentnall TA (2011) Mass spectrometry based glycoproteomics—from a proteomics perspective. *Mol Cell Proteomics* 10:R110.003251
9. Alley WR Jr, Novotny MV (2010) Glycomic analysis of sialic acid linkages in glycans derived from blood serum glycoproteins. *J Proteome Res* 9:3062–3072
10. Dell A, Morris HR (2001) Glycoprotein structure determination by mass spectrometry. *Science* 291:2351–2356
11. Peterman SM, Mulholland JJ (2006) A novel approach for identification and characterization of glycoproteins using a hybrid linear ion trap/FT-ICR mass spectrometer. *J Am Soc Mass Spectrom* 17:168–179
12. Ahn YH, Shin PM, Ji ES, Kim H, Yoo JS (2012) A lectin-coupled, multiple reaction monitoring based quantitative analysis of human plasma glycoproteins by mass spectrometry. *Anal Bioanal Chem* 402:2101–2112
13. Ahn YH, Ji ES, Shin PM, Kim KH, Kim YS, Ko JH, Yoo JS (2012) A multiplex lectin-channel monitoring method for human serum glycoproteins by quantitative mass spectrometry. *Analyst* 137:691–703
14. Matsuda A, Kuno A, Matsuzaki H, Kawamoto T, Shikanai T, Nakanuma Y, Yamamoto M, Ohkohchi N, Ikehara Y, Shoda J, Hirabayashi J, Narimatsu H (2013) Glycoproteomics-based cancer marker discovery adopting dual enrichment with *Wisteria floribunda* agglutinin for high specific glyco-diagnosis of cholangiocarcinoma. *J Proteomics* 85:1–11
15. Ferreira JA, Daniel-da-Silva AL, Alves RMP, Duarte D, Vieira I, Santos LL, Ritorino R, Amado F (2011) Synthesis and optimization of lectin functionalized nanoprobes for the selective recovery of glycoproteins from human body fluids. *Anal Chem* 83:7035–7043
16. Ahn YH, Kim YS, Ji ES, Lee JY, Jung JA, Ko JH, Yoo JS (2010) Comparative quantitation of aberrant glycoforms by lectin-based glycoprotein enrichment coupled with multiple-reaction monitoring mass spectrometry. *Anal Chem* 82:4441–4447
17. Ito S, Hayama K, Hirabayashi J (2009) Enrichment strategies for glycopeptides. *Methods Mol Biol* 534:195–203

18. Zielinska DF, Gnad F, Wiśniewski JR, Mann M (2010) Precision mapping of an in vivo N-glycoproteome reveals rigid topological and sequence constraints. *Cell* 141:897–907
19. Zhang H, Li XJ, Martin DB, Aebersold R (2003) Identification and quantification of N-linked glycoproteins using hydrazide chemistry, stable isotope labeling and mass spectrometry. *Nat Biotechnol* 21: 660–666
20. Chen R, Tan Y, Wang M, Wang F, Yao Z, Dong L, Ye M, Wang H, Zou H (2011) Development of glycoprotein capture-based label-free method for the high-throughput screening of differential glycoproteins in hepatocellular carcinoma. *Mol Cell Proteomics* 10: M110.006445
21. Wührer M, de Boer AR, Deelder AM (2009) Structural glycomics using hydrophilic interaction chromatography (HILIC) with mass spectrometry. *Mass Spectrom Rev* 28:192–206
22. Mysling S, Palmisano G, Højrup P, Thaysen-Andersen M (2010) Utilizing ion-pairing hydrophilic interaction chromatography solid phase extraction for efficient glycopeptide enrichment in glycoproteomics. *Anal Chem* 82:5598–5609
23. Qu Y, Xia S, Yuan H, Wu Q, Li M, Zou L, Zhang L, Liang Z, Zhang Y (2011) Integrated sample pretreatment system for N-linked glycosylation site profiling with combination of hydrophilic interaction chromatography and PNGase F immobilized enzymatic reactor via a strong cation exchange precolumn. *Anal Chem* 83:7457–7463
24. Ding W, Hill JJ, Kelly J (2007) Selective enrichment of glycopeptides from glycoprotein digests using ion-pairing normal-phase liquid chromatography. *Anal Chem* 79:8891–8899
25. Reusch D, Habegger M, Selman MHJ, Bulau P, Deelder AM, Wührer M, Engler N (2013) High-throughput work flow for IgG Fc-glycosylation analysis of biotechnological samples. *Anal Biochem* 432:82–89
26. Kim JY, Lee SY, Kim SK, Park SR, Kang D, Moon MH (2013) Development of an online microbore hollow fiber enzyme reactor coupled with nanoflow liquid chromatography-tandem mass spectrometry for global proteomics. *Anal Chem* 85:5506–5513
27. Wührer M, Stam JC, van de Geijn FE, Koeleman CAM, Verrips CT, Dolhain RJEM, Hokke CH, Deelder AM (2007) Glycosylation profiling of immunoglobulin G (IgG) subclasses from human serum. *Proteomics* 7:4070–4081
28. Pompach P, Brakova Z, Sanda M, Wu J, Edwards N, Goldman R (2013) Site-specific glycoforms of haptoglobin in liver cirrhosis and hepatocellular carcinoma. *Mol Cell Proteomics* 12:1281–1293
29. Schwartz I, Seger D, Shaltiel S (1999) Vitronectin. *Int J Biochem Cell Biol* 31:539–544
30. Preissner KT, Seiffert D (1998) Role of vitronectin and its receptors in haemostasis and vascular remodeling. *Thromb Res* 89:1–21
31. Preissner KT (1991) Structure and biological role of vitronectin. *Annu Rev Cell Biol* 7:275–310
32. Ogawa H, Yoneda A, Seno N, Hayashi M, Ishizuka I, Hase S, Matsumoto I (1995) Structures of the N-linked oligosaccharides on human plasma vitronectin. *Eur J Biochem* 230:994–1000
33. Sano K, Asanuma-Date K, Arisaka F, Hattori S, Ogawa H (2007) Changes in glycosylation of vitronectin modulate multimerization and collagen binding during liver regeneration. *Glycobiology* 17: 784–794
34. Lee JY, Kim JY, Park GW, Cheon MH, Kwon KH, Ahn YH, Moon MH, Lee HJ, Paik YK, Yoo JS (2011) Targeted mass spectrometric approach for biomarker discovery and validation with nonglycosylated tryptic peptides from N-linked glycoproteins in human plasma. *Mol Cell Proteomics* 10:M111.009290
35. Lee JY, Kim JY, Cheon MH, Park GW, Ahn YH, Moon MH, Yoo JS (2014) MRM validation of targeted nonglycosylated peptides from N-glycoprotein biomarkers using direct trypsin digestion of depleted human plasma. *J Proteomics* 98:206–217
36. Hua S, Hu CY, Kim BJ, Totten SM, Oh MJ, Yun N, Nwosu CC, Yoo JS, Lebrilla CB, An HJ (2013) Glyco-analytical multispecific proteolysis (Glyco-AMP): a simple method for detailed and quantitative glycoproteomic characterization. *J Proteome Res* 12:4414–4423
37. Lee HJ, Na K, Choi EY, Kim MS, Kim H, Paik YK (2010) Simple method for quantitative analysis of N-linked glycoproteins in hepatocellular carcinoma specimens. *J Proteome Res* 9:308–318
38. Song E, Pyreddy S, Mechref Y (2012) Quantification of glycopeptides by multiple reaction monitoring liquid chromatography/tandem mass spectrometry. *Rapid Commun Mass Spectrom* 26:1941–1954
39. Lee HJ, Cha HJ, Lim JS, Lee SH, Song SY, Kim H, Hancock WS, Yoo JS, Paik YK (2014) Abundance ratio-based semiquantitative analysis of site-specific N-linked glycopeptides present in the plasma of hepatocellular carcinoma patients. *J Proteome Res* 13(5):2328–2338
40. Mayampurath AM, Yu CY, Song E, Balan J, Mechref Y, Tang H (2014) Computational framework for identification of intact glycopeptides in complex samples. *Anal Chem* 86:453–463
41. Kim YJ, Zaidi-Ainouch Z, Gallien S, Domon B (2012) Mass spectrometry-based detection and quantification of plasma glycoproteins using selective reaction monitoring. *Nat Protoc* 7:859–871
42. Lim BL, Reid KB, Ghebrehiwet B, Peerschke EI, Leigh LA, Preissner KT (1996) The binding protein for globular heads of complement C1q, gC1qR. Functional expression and characterization as a novel vitronectin binding factor. *J Biol Chem* 271:26739–26744
43. Chen R, Seebun D, Ye M, Zou H, Figeys D (2014) Site-specific characterization of cell membrane N-glycosylation with integrated hydrophilic interaction chromatography solid phase extraction and LC-MS/MS. *J Proteomics* 30:194–203
44. Segu ZM, Mechref Y (2010) Characterizing protein glycosylation sites through higher-energy C-trap dissociation. *Rapid Commun Mass Spectrom* 24:1217–1225
45. Seiffert D, Loskutoff DJ (1991) Evidence that type 1 plasminogen activator inhibitor binds to the somatomedin B domain of vitronectin. *J Biol Chem* 266:2824–2830
46. Huang G, Xiong Z, Qin H, Zhu J, Sun Z, Zhang Y, Peng X, Zou J, Zou H (2014) Synthesis of zwitterionic polymer brushes hybrid silica nanoparticles via controlled polymerization for highly efficient enrichment of glycopeptides. *Anal Chim Acta* 809:61–68
47. Coligan JE, Dunn BM, Speicher DW, Wingfield PT (eds) (2001) *Current protocols in protein science*. Wiley, Hoboken
48. Shah B, Jiang XG, Chen L, Zhang Z (2014) LC-MS/MS peptide mapping with automated data processing for routine profiling of N-glycans in immunoglobulins. *J Am Soc Mass Spectrom* 25:999–1011
49. Mayampurath AM, Wu Y, Segu ZM, Mechref Y, Tang H (2011) Improving confidence in detection and characterization of protein N-glycosylation sites and microheterogeneity. *Rapid Commun Mass Spectrom* 25:2007–2019
50. Parker BL, Thaysen-Andersen M, Solis N, Scott NE, Larsen MR, Graham ME, Packer NH, Cordwell SJ (2013) Site-specific glycan-peptide analysis for determination of N-glycoproteome heterogeneity. *J Proteome Res* 12:5791–5800
51. Kronewitter SR, An HJ, de Leoz ML, Lebrilla CB, Miyamoto S, Leiserowitz GS (2009) The development of retrosynthetic glycan libraries to profile and classify the human serum N-linked glycome. *Proteomics* 9:2986–2994
52. Cao Q, Zhao X, Zhao Q, Lv X, Ma C, Zhao Y, Peng B, Ying W, Qian X (2014) Strategy integrating stepped fragmentation and glycan diagnostic ion-based spectrum refinement for the identification of core fucosylated glycoproteome using mass spectrometry. *Anal Chem* 86:6804–6811
53. Chen R, Wang F, Tan Y, Sun Z, Song C, Ye M, Wang H, Zou H (2012) Development of a combined chemical and enzymatic approach for the mass spectrometric identification and quantification of aberrant N-glycosylation. *J Proteomics* 75:1666–1674
54. Zhu J, Sun Z, Cheng K, Chen R, Ye M, Xu B, Sun D, Wang L, Liu J, Wang F, Zou H (2014) Comprehensive mapping of protein N-

- glycosylation in human liver by combining hydrophilic interaction chromatography and hydrazide chemistry. *J Proteome Res* 13:1713–1721
55. Wuhler M, Koeleman CAM, Hokke CH, Deelder CM (2006) Mass spectrometry of proton adducts of fucosylated N-glycans: fucose transfer between antennae gives rise to misleading fragments. *Rapid Commun Mass Spectrom* 20:1747–1754
56. Cheng L, Luo S, Jin C, Ma H, Zhou H, Jia L (2013) FUT family mediates the multidrug resistance of human hepatocellular carcinoma via the PI3K/Akt signaling pathway. *Cell Death Dis* 4:e923. doi:10.1038/cddis.2013.450
57. Kang X, Wang N, Pei C, Sun L, Sun R, Chen J, Liu Y (2012) Glycan-related gene expression signatures in human metastatic hepatocellular carcinoma cells. *Exp Ther Med* 3:415–422
58. Nakagawa T, Uozumi N, Nakano M, Mizuno-Horikawa Y, Okuyama N, Taguchi T, Gu J, Kondo A, Taniguchi N, Miyoshi E (2006) Fucosylation of N-glycans regulates the secretion of hepatic glycoproteins into bile ducts. *J Biol Chem* 281:29797–29806
59. Shah N, Kuntz DA, Rose DR (2008) Golgi alpha-mannosidase II cleaves two sugars sequentially in the same catalytic site. *Proc Natl Acad Sci U S A* 105:9570–9575
60. Mayampurath AM, Song E, Mathur A, Yu C, Hammoud ZT, Mechref Y, Tang H (2014) Label-free glycopeptide quantification for biomarker discovery in human sera. *J Proteome Res* 13. doi: 10.1021/pr500242m
61. Zhu Z, Hua D, Clark DF, Go EP, Desaire H (2013) GlycoPep detector: a tool for assigning mass spectrometry data of N-linked glycopeptides on the basis of their electron transfer dissociation spectra. *Anal Chem* 85:5023–5032
62. Wei T, Liu Q, He F, Zhu W, Hu L, Guo L, Zhang J (2012) The role of N-acetylglucosaminyltransferases V in the malignancy of human hepatocellular carcinoma. *Exp Mol Path* 93(1):8–17
63. Yanagi M, Aoyagi Y, Suda T, Mita Y, Asakura H (2001) N-acetylglucosaminyltransferase V as a possible aid for the evaluation of tumor invasiveness in patients with hepatocellular carcinoma. *J Gastroenterol Hepatol* 16(11):1282–1289